Journal of the American Heart Association

ORIGINAL RESEARCH

Vascular Stiffening Mediated by Rho-Associated Coiled-Coil Containing Kinase Isoforms

Yuxin Li, MD, PhD*; Haw-Chih Tai, PhD*; Nikola Sladojevic, MD, PhD; Hyung-Hwan Kim, PhD; James K. Liao, MD

BACKGROUND: The pathogenesis of vascular stiffening and hypertension is marked by non-compliance of vessel wall because of deposition of collagen fibers, loss of elastin fibers, and increased vascular thickening. Rho/Rho-associated coiled-coil containing kinases 1 and 2 (ROCK1 and ROCK2) have been shown to regulate cellular contraction and vascular remodeling. However, the role of ROCK isoforms in mediating pathogenesis of vascular stiffening and hypertension is not known.

METHODS AND RESULTS: Hemizygous *Rock* mice (*Rock1*$^{+/-}$ and *Rock2*$^{+/-}$) were used to determine the role of ROCK1 and ROCK2 in age-related vascular dysfunction. Both ROCK activity and aortic stiffness increased to a greater extent with age in wild-type mice compared with that of *Rock1*$^{+/-}$ and *Rock2*$^{+/-}$ mice. As a model for age-related vascular stiffening, we administered angiotensin II (500 ng/kg per minute) combined with nitric oxide synthase inhibitor, L-N$^{\omega}$-nitroarginine methyl ester (0.5 g/L) for 4 weeks to 12-week-old male *Rock1*$^{+/-}$ and *Rock2*$^{+/-}$ mice. Similar to advancing age, angiotensin II/L-N$^{\omega}$-nitroarginine methyl ester caused increased blood pressure, aortic stiffening, and vascular remodeling, which were attenuated in *Rock2*$^{+/-}$, and to a lesser extent, *Rock1*$^{+/-}$ mice. The reduction of aortic stiffening in *Rock2*$^{+/-}$ mice was accompanied by decreased collagen deposition, relatively preserved elastin content, and less aortic wall hypertrophy. Indeed, the upregulation of collagen I by transforming growth factor-β1 or angiotensin II was greatly attenuated in *Rock2*$^{-/-}$ mouse embryonic fibroblasts.

CONCLUSIONS: These findings indicate that ROCK1 and ROCK2 mediate both age-related and pharmacologically induced aortic stiffening, and suggest that inhibition of ROCK2, and to a lesser extent ROCK1, may have therapeutic benefits in preventing age-related vascular stiffening.

Key Words: aging ■ aortic stiffness ■ eEF1A1 ■ Rho kinase ■ vascular remodeling

Epidemiological studies have shown that vascular stiffening and systolic hypertension are independent predictors of cardiovascular disease.[1,2] Although there is a close association between aortic stiffness and the development of systemic hypertension,[3,4] the mechanisms leading to vascular stiffening and the temporal relationship between aortic stiffness and the development of hypertension remains unclear. Nevertheless, the pathogenesis of age-related vascular stiffening with or without hypertension is marked by non-compliance of the vessel wall because of deposition of non-compliant collagen fibers, loss or fragmentation of elastin fibers, endothelial dysfunction, and increased vascular matrix remodeling.[5,6] Therefore, signaling pathways, which affect the compliance and contractility of the vessel wall, may be important contributors to the pathogenesis of vascular stiffening.

The Rho/Rho-associated coiled-coil containing kinases (ROCK1 and ROCK2) are important mediators of vascular function through their regulation of

Correspondence to: James K. Liao, MD, Section of Cardiology, Department of Medicine, University of Chicago, 5841 S. Maryland Avenue, MC6080, B608, Chicago, IL 60637. E-mail: jliao@medicine.bsd.uchicago.edu

†Y. Li and H.-C. Tai contributed equally and are co-first authors.

Supplementary Material for this article is available at https://www.ahajournals.org/doi/suppl/10.1161/JAHA.121.022568

For Sources of Funding and Disclosures, see page 13.

JAHA is available at: www.ahajournals.org/journal/jaha

CLINICAL PERSPECTIVE

What Is New?

- Aortic Rho/Rho-associated coiled-coil containing kinases (ROCK) activity increases with vascular age.
- ROCK is an important mediator of aortic stiffness in aging mice.
- Loss of Rock2 attenuates hypertension, aortic stiffening, vascular remodeling, and fibrosis in a pharmacologic model of aortic stiffening.

What Are the Clinical Implications?

- Inhibition of ROCK, especially ROCK2, may have therapeutic benefits in preventing age-related aortic stiffening.
- ROCK2 mediates smooth muscle cell proliferation and profibrotic gene expression, suggesting ROCK2 is a critical mediator of age-associated vascular remodeling.

Nonstandard Abbreviations and Acronyms

Ang II	angiotensin II
CTGF	connective tissue growth factor
eEF1A1	eukaryotic elongation factor 1-alpha 1
eNOS	endothelial nitric oxide synthase
L-NAME	L-N$^{\omega}$-nitroarginine methyl ester
MEF	mouse embryonic fibroblasts
MLC	myosin light chain
PWV	pulse wave velocity
ROCK1	Rho/Rho-associated coiled-coil containing kinase 1
ROCK2	Rho/Rho-associated coiled-coil containing kinase 2
SMC	smooth muscle cells
TGF-β1	transforming growth factor β1
VSMC	vascular smooth muscle cells
WT	wild-type

actin cytoskeleton, cellular contraction, and fibrosis.[7,8] Clinically, we have shown that increased leukocyte ROCK activity is associated with advancing age, systolic hypertension, and increased carotid-femoral pulse wave velocity (PWV).[9,10] Recently, we identified eukaryotic elongation factor 1-alpha 1 (eEF1A1), a regulator of cellular protrusion[11] and proliferation,[12] as a binding partner for ROCK2.[13] Subsequent mutational analysis of eEF1A1 identified Thr^{432} as the specific ROCK2 phosphorylation site. Furthermore, ROCK affects cardiovascular remodeling through its effects on neointima formation[14] and regulation of transforming growth factor-β1 (TGF-β1), connective tissue growth factor (CTGF), and procollagen expression.[15,16] These findings suggest that ROCK could be a critical mediator of the mechanical properties of the vascular wall.

Previous studies with ROCK inhibitors are limited by their relative lack of specificity for ROCK as opposed to other serine/threonine protein kinases such as PKA, protein kinase C, and citron kinase when given in vivo, and are unable to distinguish between the actions of specific ROCK isoforms.[17] Hence, a genetic approach using haploinsufficiency of specific ROCK isoforms is needed to determine the role of ROCK isoforms in vascular diseases. In this study, we used hemizygous *Rock1*$^{+/-}$ and *Rock2*$^{+/-}$ mice to investigate the role of ROCK isoforms in the pathogenesis of vascular stiffening.

METHODS

The data, analytic methods, and study materials are available upon request.

Animals

The hemizygous *Rock* mice, *Rock1*$^{+/-}$ and *Rock2*$^{+/-}$ mice, were generated as described.[14] Wild-type (WT) littermates were used as the controls for *Rock1*$^{+/-}$ or *Rock2*$^{+/-}$ mice. All mice are congenic strains on a C57Bl/6J background. Mice were housed on a 12-hours light/dark cycle in a specific pathogen-free facility maintained by the University of Chicago Animal Resources Center. Standard laboratory diet and drinking water were supplied ad libitum. For all surgical procedures, animals were anesthetized with 2% isoflurane and rectal temperature was monitored and maintained at 37 °C ±0.5 °C. The level of anesthesia was monitored with pedal reflex. The analgesic buprenorphine (0.1–0.2 mg/kg) was administered subcutaneously at the beginning of surgery and once every 12 hours for 4 days or until animals are observed to be free of signs of pain. All animals were euthanized by carbon dioxide (CO_2) asphyxiation. A gradual fill method was used with a displacement rate of 10% to 30% of the chamber volume/minute (3 L/min). CO_2 flow was continued for at least 1 minute after respiratory arrest. Cervical dislocation, a secondary euthanasia method was used for all the animal procedures. All animal protocols were approved by the Institutional Animal Care and Use Committee at the University of Chicago and conform to National Institutes of Health guidelines.

Western Blotting

Protein was extracted from tissues or cells as previously described.[18] The same amount of extracted protein was loaded on SDS-PAGE gel and transferred to polyvinylidene difluoride membranes (Immobilon-P;

Millipore). The membranes were blocked with 3% bovine serum albumin (A7906; Sigma-Aldrich) and 0.1% Tween-20 (B1379; Sigma-Aldrich) in tris buffered saline for 1 hour at room temperature and then incubated overnight at 4 °C with primary antibodies (Table S1). After incubated with corresponding secondary antibodies at room temperature for 1 hour, the regions containing proteins were visualized by the enhanced chemiluminescence kit (Clarity Western ECL Substrate; Bio-Rad). Densitometric analysis was performed using ImageJ Software (National Institutes of Health). Densitometric readings of band intensities were normalized to control protein expression levels.

RNA Isolation and Quantitative Real-Time Polymerase Chain Reaction

Total RNA was extracted from tissues or cells, using the PureLink RNA Mini Kit (Invitrogen), according to the manufacturer's instructions. Total RNA was converted to cDNA using the iScript Reverse Transcription Supermix Kit (Bio-Rad). The PowerUp SYBR Green Master Mix (Applied Biosystems) was used to perform amplifications on the StepOnePlus Real-Time PCR System (Applied Biosystems). The Ct value calculated by the StepOne Software version 2.3 (Applied Biosystems) for all samples was normalized to the housekeeping gene, *Hprt*. The relative fold change was computed by the ΔΔCt method. The primers used in this study are listed in Table S2.

Ang II/L-NAME Administration

Twelve-week-old male WT, *Rock1*$^{+/-}$, and *Rock2*$^{+/-}$ mice were implanted with Alzet osmotic mini-pump (Model 1004) containing saline or angiotensin II (Ang II) (500 ng/kg per minute, A9525; Sigma-Aldrich). Mice were anesthetized with 2% isoflurane and analgesic buprenorphine (0.1–0.2 mg/kg) was administered subcutaneously before implantation of the osmotic mini-pump. A 1.0-cm vertical mid-scapular skin incision was made, followed by a creation of a 3.5-cm deep subcutaneous pocket. The osmotic mini-pump was inserted into the pocket. Skin closure was performed using 4-0 silk sutures, and mice were allowed to recover on a heating plate at 37 °C. The L-N$^{\omega}$-nitroarginine methyl ester (L-NAME, 0.5 g/L, N5751; Sigma-Aldrich) was supplied in the drinking water. The duration of treatment was 4 weeks. Measurements of aortic stiffness and blood pressure (BP) were performed at baseline and at 4 weeks after treatment.

Measurements of PWV, Blood Pressure, and Hemodynamic Parameters in Mice

Mice were anesthetized with 2% isoflurane on a heating (37 °C) board with integrated ECG electrodes. The pulse waveforms in the aortic root and abdominal aorta were obtained by pulse wave Doppler ultrasonography (Vevo 2100 imaging system, VisualSonics) and synchronized with ECG monitoring. The pulse wave, aortic dimensions in systole and diastole were measured by 38-MHz transducer. The PWV was calculated by dividing the distance by the difference of transit time between aortic root and abdominal aorta. Invasive blood pressure was measured using a Millar pressure catheter (1.4F, model SPR-671 recorded on MPVS-300 System) inserted into the aortic root of mice under 2% isoflurane anesthesia. In Ang II/L-NAME treated mice, a second pressure transducer was inserted via the right femoral artery and advanced into the thoracic aorta. The pullback procedure was performed to simultaneously measure PWV, determine the transit distance, and correct for differences in frequency response and amplifier delays between the 2 pressure transducers.[19] The pressure waveforms in the aorta were recorded and analyzed to obtain systolic, diastolic, and mean aortic blood pressure (systolic BP, diastolic BP, and mean BP, respectively). These parameters were used to calculate pulse pressure, the change in pressure from augmentation point to peak systolic pressure (ΔP), and the augmentation index [(ΔP/pulse pressure)×100]. The aortic systolic and diastolic internal and outer diameter were determined by ultrasonography, and the corresponding lumen area and wall thickness were calculated. Using pulse wave Doppler ultrasonography, the flow velocity waveform and diameter at the left ventricular outflow tract (LVOT) and aortic root were measured. The LVOT area was calculated by measuring the average diameter, assuming a circular orifice. The LVOT flow velocity waveform was multiplied by LVOT area to derive the flow volume in the LVOT, which is equivalent to flow volume in the aorta.

Histological Analysis

Mice were anesthetized with 2% isoflurane and euthanized by CO_2 inhalation. At the time of euthanizing, the left ventricle of euthanized mouse was cannulated and perfused with PBS containing heparin. The aorta was then perfused and fixed with 4% paraformaldehyde in PBS under physiological pressure. Following removal of the aorta and further incubation in 4% paraformaldehyde in PBS for 6 hours, the aortic segments are embedded in optimal cutting temperature compound and frozen. Ten sequential cross-sections of 5-μm thickness at 3- to 4-mm intervals distal to the aortic valve were obtained for immunohistochemical and morphometric analysis. Fresh frozen sections were cut on a freezing microtome (Microm; Walldorf). Slides were stained with hematoxylin and eosin, elastin, picosirius red, and cross-sectional images were analyzed using an image analysis system (Multiscan; Fullerton). The identity of each sample was

coded to allow data to be analyzed in a "blinded" manner. Measurements of vessel thickness and medial area were determined on cross-sections of aortas on the same slide used for morphometric analysis. Wall thickness was determined in pressure-perfusion fixed aortas (at mean BP of 100 mm Hg). Medial area was determined by elastin stain and defined as the area between the internal and external elastic lamina. The medial areas were measured using National Institutes of Health Image software and the average medial area was calculated. To correct for vessel deformation and off-transverse sectioning, the areas were determined by measuring the circumference of the vessel lumen and calculating the area as a generalized circle based on the measured circumference. For morphometric analysis, sections were stained with picosirius red (24901; Polysciences Inc.) for collagen, and elastin stain for elastin (HT25; Sigma-Aldrich). The areas of collagen and elastin staining were then standardized to medial area or wall thickness.

Measurement of Hydroxyproline and Desmosine Content

The entire aorta was harvested and snap freezing in liquid nitrogen. The aortic tissues were hydrolyzed in 6 N HCl at 100 °C for 24 hours as described.[20] The amount of cross-linked collagen was quantitated by measuring the amount of hydroxyproline in aortic lysates as described.[21] The amount of desmosine and isodesmosine, which forms cross-links with elastin, was determined by high performance liquid chromatography/mass spectrometry as described.[20] The amount of collagen and elastin were standardized to vessel length (mm). The ratio of hydroxyproline to desmosine and isodesmosine was taken as an index of vascular remodeling.

Isolation of Mouse Primary Aortic Smooth Muscle Cells

Primary aortic smooth muscle cells (SMC) were isolated from 8- to 10-week-old mice. The thoracic aortas were dissected from the arch to just above the diaphragm. The adventitia and the surrounding adipose tissue were carefully removed. Aorta was cut longitudinally and the endothelial layer was gently removed by sterile cotton swab. The luminal side of aorta was attached to gelatin-coated 35-mm culture dish with growth medium. The dishes were placed in 37 °C and 5% CO_2 incubator and left undisturbed for 5 days, allow the aortic SMC to migrate and proliferate from the aorta. The growth media containing DMEM/F12 (11320033), 20% fetal bovine serum (FBS), Smooth Muscle Growth Supplement (S00725), 1% GlutaMAX (35050061) and 1% Antibiotic-Antimycotic (15240062) were used for the SMC culture. All the cell culture reagents listed above were purchased from Thermo Fisher Scientific and were used according to the manufacturer's instructions. Primary SMC between passages 3 to 6 were used for all experiments. The mRNA levels of SMC differentiation markers (*Myh11* and *Smtn*) and stem cell markers (*S100b* and *Sca1*) were significantly lower in SMC compared with aortas, suggesting SMC exhibit proliferative phenotype (data not shown). For in vitro studies, SMC were serum (1%)-starved overnight and then treated with or without 20 μmol/L ROCK inhibitor Y-27632 (688001; Millipore) for 1 hour before stimulation with 1 μmol/L Ang II (A9525; Sigma-Aldrich) for 24 hours.

Transfection of Small Interfering RNA

Control small interfering RNA (siRNA) (sc-37007), *Rock1* siRNA (sc-36432), and *Rock2* siRNA (sc-36432) were purchased from Santa Cruz Biotechnology. The siRNAs were diluted to 20 nmol/L in Opti-MEM (31985070; Thermo Fisher) and mixed with Lipofectamine RNAiMax (13778075; Thermo Fisher) at room temperature for 20 minutes. Mouse primary aortic SMC were seeded at subconfluent densities in collagen type I-coated 6-well plates or 60-mm culture dishes in growth media without antibiotics. The siRNA-Lipofectamine mixtures were added to SMC and incubated for 48 hours.

SMC Proliferation and Protein Synthesis Assay

Mouse aortic SMC in logarithmic growth phase were harvested and plated at 1.5×10^5 cells/cm^2 and cultured overnight in DMEM with 10% FBS. SMC were transfected the following day with control vector, WT eEF1A1 cDNA vector or the mutant eEF1A1 (ΔT432A) cDNA vector, which cannot be phosphorylated by ROCK2. After transfection for 48 hours, SMC were synchronized to G0 with serum-starvation for 16 hours. SMC proliferation was assessed by cell count and [^{3}H]-thymidine uptake and protein synthesis by [^{3}H]-leucine (New England Nuclear-Life Science Products) uptake in response to 10% FBS. SMC were treated with the indicated conditions in the presence of diluents, [^{3}H]-thymidine or [^{3}H]-leucine (1 μCi/mL) for 24 hours. After incubating at room temperature for 45 minutes, cellular proteins were precipitated with 5% trichloroacetic acid, resuspended in 0.4 N NaOH, and the radioactivity was counted in a scintillation counter (Beckman LS 6000IC). Transfection efficiency was 30% to 35% and standardized to transfection with β-gal cDNA. The results were expressed as counts per minute (cpm) per microgram protein.

Isolation and Immortalization of Mouse Embryonic Fibroblasts

Primary mouse embryonic fibroblasts (MEF) were cultured from 13-day-old embryos derived from WT,

Rock1$^{-/-}$, and *Rock2*$^{-/-}$ mice. The embryos were separated from their yolk sac and placed in the complete growth medium, DMEM with 10% FBS, 1% penicillin and streptomycin, and 1% GlutaMAX (Invitrogen). After the embryonic head and innards were removed, the trunk was homogenized and trypsinized at 37 °C for 45 minutes. After neutralizing the trypsin with the complete growth medium, the MEF were isolated from the remaining embryonic body by repeated pipetting and cultured until confluent. After the third passage, the MEF from each strain were immortalized by infection with a retrovirus vector expressing SV40 large T antigen, using neomycin selection for 2 weeks. MEF were cultured in gelatin-coated dishes. After serum starvation overnight, MEF were cotreated with or without ROCK inhibitor Y-27632 (20 μmol/L; 688001, Millipore) and stimulated for 24 hours with TGF-β1 (10 ng/mL; 100-21C, PeproTech).

Statistical Analysis

All results are expressed as the mean±SEM. Comparisons of parameters were performed with 1-way ANOVA followed by post-hoc Tukey Honest Significant Difference test for multiple comparisons. Statistical significance was evaluated with GraphPad Prism 7 (GraphPad Software) and JMP 7 (SAS Institute Inc.). A P value of <0.05 was considered to be statistically significant.

RESULTS

Effects of Age on ROCK Activity

Age is associated with increased aortic stiffening and systolic hypertension.[22] To determine whether increased ROCK expression and activity are associated with aging in mice, we measured ROCK activity and expression in the aortas of 4-, 11-, and 20-month-old male WT C57BL/6J mice. Compared with 4-month-old mice, 11- and 20-month-old mice exhibited increased aortic ROCK activity (P<0.001 for both, n=6 in each group) as determined by phosphorylation of myosin-binding subunit of myosin light chain (MLC) phosphatase (Figure 1A and 1B). Interestingly, there was no increase in ROCK1 or ROCK2 expression in aortas of 11- and 20-month-old mice (Figure 1C). These findings suggest that aging may lead to conditions, which increases ROCK activity but not ROCK expression in the aorta.

Effects of ROCK Isoforms on Age-Associated Aortic Stiffness

To investigate the involvement of ROCK isoforms in age-related aortic stiffening, we measured PWV in mice at 4, 11, and 20 months of age. The age-associated increase in aortic ROCK activity correlated with greater aortic stiffness in 11 and 20-month-old male WT mice compared with that of 4-month-old male WT mice (PWV at 11 and 20 months: 6.43±0.18 and 7.08±0.23 versus 4 months: 4.13±0.17 m/s; P<0.001 for both compared with 4 months, n=6 in each group) (Figure 1D). Interestingly, in 4-month-old male mice, aortic stiffness was slightly less in *Rock1*$^{+/-}$ and *Rock2*$^{+/-}$ mice compared with that of WT mice (PWV, 3.42±0.16 and 3.23±0.13 m/s versus 4.13±0.17 m/s; P=0.04 and P=0.003, respectively, n=6 in each group). Similar to 20-month-old WT mice, aortic stiffness was greater in 20-month-old male *Rock1*$^{+/-}$ and *Rock2*$^{+/-}$ mice compared with that of 4-month-old male *Rock1*$^{+/-}$ and *Rock2*$^{+/-}$ mice (PWV at 20 months: 5.11±0.16 and 4.33±0.08 m/s, PWV at 4 months: 3.42±0.16 and 3.23±0.13 m/s, respectively; P<0.001 for both compared with corresponding 4-month-old mice, n=6 in each group), but the magnitude of increase was much less compared with that of 20-month-old WT mice (P<0.001 for both) with 20-month-old *Rock2*$^{+/-}$ mice being the most attenuated (WT: 7.08±0.23 versus *Rock2*$^{+/-}$: 4.33±0.08 m/s; P<0.001, n=6 in each group). Indeed, aortic stiffness in 20-month-old *Rock2*$^{+/-}$ mice was not different compared with that of 4-month-old WT mice (PWV, 4.33±0.08 m/s versus 4.13±0.17 m/s; P>0.05, n=6 in each group), suggesting that haploinsufficiency of *Rock2* abrogates age-related aortic stiffness. Similar findings of aortic stiffness were obtained when comparing 4-month-old and 11-month-old female WT littermates and hemizygous *Rock1*$^{+/-}$ and *Rock2*$^{+/-}$ mice (Figure 1E). These findings indicate that haploinsufficiency of *Rock1*, and to a greater extent, of *Rock2*, attenuates age-associated aortic stiffness.

Effects of ROCK Isoforms on Age-Associated Changes in Endothelial Nitric Oxide Synthase and Extracellular Matrix

We next determine the effects of ROCK isoforms on age-associated changes in endothelial nitric oxide synthase (eNOS) expression and extracellular matrix in aortas of 4 and 12-month-old male WT littermate, and hemizygous *Rock1*$^{+/-}$ and *Rock2*$^{+/-}$ mice. The expression of eNOS was similar between 4-month-old WT, *Rock1*$^{+/-}$ and *Rock2*$^{+/-}$ mice (Figure 1F). However, compared with 4-month-old mice, eNOS expression was decreased by 64% and 60% in 12-month-old WT and *Rock1*$^{+/-}$ mice (P<0.001 for both, n=5 in each group), respectively, whereas there were no changes in eNOS expression between 4 and 12-month-old *Rock2*$^{+/-}$ mice (P>0.05, n=5 in each group). These findings suggest that *Rock2* mediates the downregulation of eNOS expression during vascular aging.

In 4-month-old male mice, the hydroxyproline and desmosine content in the thoracic aortas were similar between WT, *Rock1*$^{+/-}$ and *Rock2*$^{+/-}$ mice (Figures 1G and 1H). However, in 12-month-old mice, the hydroxyproline

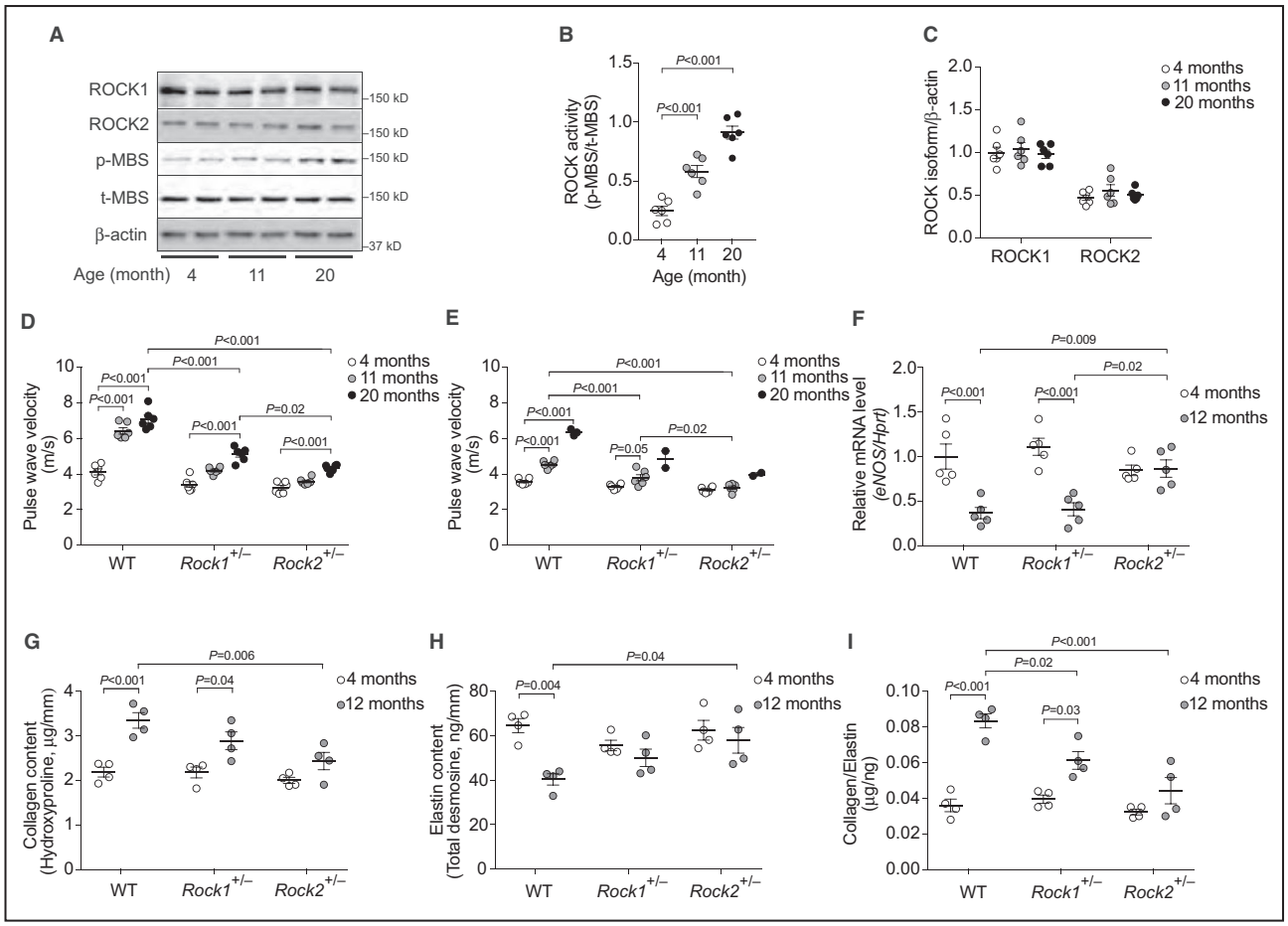

Figure 1. Rho/Rho-associated coiled-coil containing kinase (ROCK) isoform expression and activity with age and their effects on age-related aortic wall remodeling and stiffness.

A, Representative immunoblots showing the protein level of ROCK isoforms, phosphorylated myosin-binding subunit, total myosin-binding subunit, and β-actin in aortas of 4, 11, and 20 months of age male C57BL/6J mice. Densitometric analysis of (**B**) ROCK activity (phosphorylated myosin-binding subunit/total myosin-binding subunit) and (**C**) ROCK expression (standardized to β-actin) in aortas of 4, 11, and 20 months of age male wild-type (WT) mice, n=6 aortas in each group. Pulse wave velocity in the aortas of 4, 11 and 20 months of age (**D**) male and (**E**) female WT littermates, *Rock1*$^{+/-}$, and *Rock2*$^{+/-}$ mice. For male mice: n=6 mice in all groups. For female mice: n=6 mice in all 4 and 11-month-old groups, n=3 mice in 20-month-old WT group, n=2 mice in 20-month-old *Rock1*$^{+/-}$ and *Rock2*$^{+/-}$ groups. **F**, The mRNA level of endothelial nitric oxide synthase in aortas of 4- and 12-month-old male WT, *Rock1*$^{+/-}$, and *Rock2*$^{+/-}$ mice, n=5 aortas in each group. **G**, Collagen and (**H**) elastin content in aortas of 4- and 12-months-old male WT, *Rock1*$^{+/-}$, and *Rock2*$^{+/-}$ mice. The collagen and elastin content were determined by quantification of hydroxyproline and total desmosine; n=4 aortas in all groups. **I**, The ratio of collagen (hydroxyproline) to elastin (desmosine) in the aorta; n=4 aortas in all groups. Results are expressed as mean±SEM. *P* values were calculated using 1-way ANOVA with Tukey Honest Significant Difference test. p-MBS indicates phosphorylated myosin-binding subunit; ROCK/*Rock*, Rho/Rho-associated coiled-coil containing kinase; t-MBS, total myosin-binding subunit; eNOS, endothelial nitric oxide synthase; Hprt, hypoxanthine phosphoribosyltransferase; and WT, wild-type.

content was increased in aortas of WT and *Rock1*$^{+/-}$ mice, but not in the aortas of *Rock2*$^{+/-}$ mice (Figure 1G). In contrast, the reduced aortic desmosine or elastin content in 12-month-old WT mice was not observed in aortas of corresponding age *Rock1*$^{+/-}$ and *Rock2*$^{+/-}$ mice (Figure 1H). Consequently, the increased ratio of collagen to elastin in 12-month-old WT and *Rock1*$^{+/-}$ aortas was substantially attenuated in 12-month-old *Rock2*$^{+/-}$ aortas (Figure 1I). These findings indicate that *Rock2* mediates age-associated aortic fibrosis, which could account for the increased pulse pressure and stiffness with age.

ROCK Isoforms Mediate Pharmacologically-Induced Vascular Stiffening

To determine the hemodynamic and histological effects of *Rock1* and *Rock2* on age-associated aortic stiffening, we used a pharmacologically-induced model of vascular stiffening to induce age-like vascular changes in mice.[20] Accordingly, 12-week-old male WT, *Rock1*$^{+/-}$ and *Rock2*$^{+/-}$ mice were treated with Ang II (500 ng/kg per minute) and L-NAME (0.5 g/L) for 4 weeks. With saline and Ang II/L-NAME treatment, body weights

were not different between the groups of mice (Table). However, treatment with Ang II/L-NAME increased the heart weights as well as the heart weight to body weight ratios of WT and *Rock1*$^{+/-}$ mice to a greater extent compared with that of *Rock2*$^{+/-}$ mice. These findings indicate that treatment with Ang II/L-NAME increased myocardial hypertrophy in WT and *Rock1*$^{+/-}$ mice, but to a lesser extent, in *Rock2*$^{+/-}$ mice. Indeed, systolic BP and mean BP were substantially increased with Ang II/L-NAME treatment in WT and *Rock1*$^{+/-}$ mice, and to a much lesser extent, in *Rock2*$^{+/-}$ mice (Table).

The pressure waveforms of invasive blood pressure monitoring showed that the increases in pulse pressure, ΔP, and augmentation index following Ang II/L-NAME treatment in WT mice were attenuated in *Rock1*$^{+/-}$ mice, and more substantially reduced in *Rock2*$^{+/-}$ mice (Figure 2A through 2C). This correlated with greater distensibility as measured by changes in the difference between systolic and diastolic internal diameters in the aortic root of *Rock2*$^{+/-}$ mice compared with that of WT and *Rock1*$^{+/-}$ mice (Figure 2D through 2F). Compared with control (saline), aortic wall thickness in WT and *Rock1*$^{+/-}$ mice was also increased with treatment of Ang II/L-NAME, but this thickening of the aortic wall was absent in *Rock2*$^{+/-}$ mice (Figure 2G). These findings suggest greater distensibility or elasticity of aortas from *Rock2*$^{+/-}$ mice compared with that of WT and *Rock1*$^{+/-}$ mice.

Using ultrasonography and pulse wave Doppler to measure the diameter of left ventricular outflow tract (LVOT) and the peak and mean velocities through LVOT, we calculated the peak and mean flow in LVOT. The diameter of LVOT for all groups were similar and did not change with Ang II/LNAME treatment (Table). However, peak LVOT velocities were higher in *Rock2*$^{+/-}$ mice, both with saline and Ang II/L-NAME treatment, suggesting higher flow across LVOT. Indeed, treatment with Ang II/L-NAME decreased peak and mean flow in WT mice, but had little or no effect on these parameters in *Rock1*$^{+/-}$ and *Rock2*$^{+/-}$ mice. This corresponded to a smaller and no increase in PWV in Ang II/L-NAME-treated *Rock1*$^{+/-}$ and *Rock2*$^{+/-}$ mice, respectively, compared with that of WT mice (PWV: WT, 4.93±0.06 m/s; *Rock1*$^{+/-}$, 4.16±0.10 m/s; *Rock2*$^{+/-}$, 3.25±0.03 m/s, $P<0.001$ compared with WT mice, Figure 2H). These results suggest that *Rock1*, and to a greater extent *Rock2*, plays an important role in regulating aortic distensibility and flow.

Effects of ROCK on Aortic Hypertrophy and Vascular Remodeling

Next, we examined the morphology and extracellular matrix of aortas from WT and *Rock* mutant mice. Using hematoxylin and eosin staining, we found that treatment with Ang II/L-NAME increased the medial area of the aortic wall, as determined by the area between the internal and external elastic lamina. This increase in medial area was smaller in *Rock2*$^{+/-}$ mice compared with that of WT mice (Figure 3A and 3B). Indeed, treatment with Ang II/L-NAME increased aortic wall thickness by ultrasonography in WT mice, which was attenuated

Table 1. Hemodynamic Parameters of Aorta in Ang II/L-NAME Treated Hemizygous ROCK Mice

	WT		*Rock1*$^{+/-}$		*Rock2*$^{+/-}$	
	Saline (n=4)	Ang II/L-NAME (n=5)	Saline (n=3)	Ang II/L-NAME (n=3)	Saline (n=3)	Ang II/L-NAME (n=4)
Body weight, g	21.8±0.3	22.2±0.2	21.9±0.2	22.1±0.3	22.0±0.3	22.4±0.2
Heart weight, mg	102.7±0.5	134.1±0.9‡	102.9±1.0	132.8±1.1‡	102.8±1.7	118.9±1.0‡¶
Heart weight/body weight, mg/g	4.7±0.1	6.1±0.1‡	4.7±0.1	6.0±0.1‡	4.7±0.1	5.3±0.1†¶
Hemodynamics						
Heart rate, beats/min	379.5±10.4	382.2±7.7	370.7±11.4	379.7±13.6	390.0±14.8	383.3±9.8
sBP, mm Hg	117.3±1.3	135.2±1.7‡	114.0±1.7	129.3±3.0‡	112.7±1.8	120.0±1.5¶
dBP, mm Hg	82.5±1.6	89.2±1.3*	81.7±1.5	89.3±2.2*	80.0±1.5	85.8±1.1
mBP, mm Hg	94.0±0.9	104.6±0.6‡	92.7±1.5	102.3±2.3‡	90.7±0.3	97.0±1.1*‖
Aortic hemodynamics						
Peak LVOT velocity, cm/s	106.1±4.5	86.7±3.4*	105.2±5.9	89.1±3.3	125.7±5.4	117.1±4.4¶
Diameter of LVOT, cm	0.085±0.002	0.084±0.002	0.085±0.002	0.086±0.002	0.082±0.003	0.084±0.002
Peak flow, cm^3/s	0.605±0.026	0.486±0.019*	0.600±0.028	0.517±0.031	0.666±0.026	0.644±0.018‖
Mean flow, cm^3/s	0.149±0.003	0.136±0.003†	0.146±0.002	0.143±0.002	0.157±0.003	0.161±0.002¶

Twelve-week-old, male wild-type littermates, *Rock1*$^{+/-}$, and *Rock2*$^{+/-}$ mice were treated with angiotensin II (500 ng/kg per minute) and L-N$^{\omega}$-nitroarginine methyl ester (L-NAME; 0.5 g/L, drinking water) for 4 weeks. Results are expressed as mean±SEM. *P* values were calculated using 1-way ANOVA with Tukey Honest Significant Difference test. Ang II indicates angiotensin II; dBP, diastolic blood pressure; L-NAME, L-N$^{\omega}$-nitroarginine methyl ester; LVOT, left ventricular outflow tract; mBP, mean blood pressure; *Rock*, Rho/Rho-associated coiled-coil containing kinase; and sBP, systolic blood pressure.

*$P<0.05$, †$P<0.01$, ‡$P<0.001$ compared with saline.

‖$P<0.01$, ¶$P<0.001$ compared with corresponding treatment of wild-type mice.

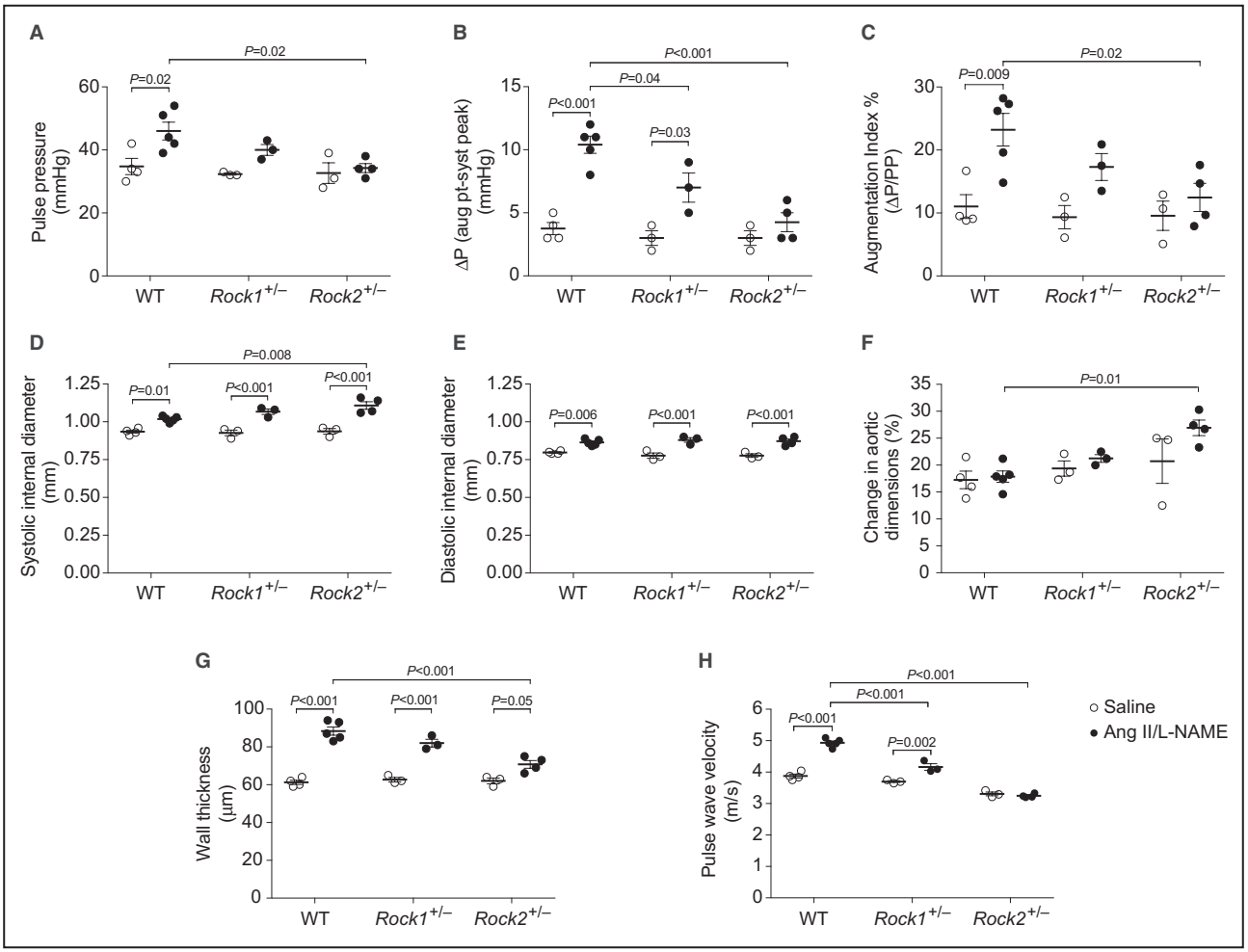

Figure 2. Hemodynamic parameters in Angiotensin II/L-N$^{\omega}$-nitroarginine methyl ester–treated hemizygous *Rock* mice. Twelve-week-old, male wild-type littermates, *Rock1*$^{+/-}$, and *Rock2*$^{+/-}$ mice were treated with angiotensin II (Ang II; 500 ng/kg per minute) and L-N$^{\omega}$-nitroarginine methyl ester (L-NAME, 0.5 g/L, drinking water) for 4 weeks. **A**, Pulse pressure, (**B**) ΔP, augmentation point to peak systolic pressure, and (**C**) augmentation index were obtained by pressure waveforms from pressure transducers in the aorta. **D**, Systolic internal diameter, (**E**) diastolic internal diameter, (**F**) change in the systolic and diastolic internal diameters of the aortic root, and (**G**) aortic wall thickness were determined by ultrasonography. **H**, Pulse wave velocity was determined by pressure waveforms in aortic root and abdominal aorta at the level of renal artery. Saline group: wild-type (n=4), *Rock1*$^{+/-}$ (n=3), and *Rock2*$^{+/-}$ (n=3); Ang II/L-N$^{\omega}$-nitroarginine methyl ester group: wild-type (n=5), *Rock1*$^{+/-}$ (n=3), and *Rock2*$^{+/-}$ (n=4). Results are expressed as mean±SEM. *P* values were calculated using 1-way ANOVA with Tukey Honest Significant Difference test. Ang II indicates angiotensin II; PP, pulse pressure; ΔP, augmentation point to peak systolic pressure; *Rock*, Rho/Rho-associated coiled-coil containing kinase; and WT, wild-type.

in *Rock1*$^{+/-}$ mice, and to a greater extent, in *Rock2*$^{+/-}$ mice (Table). This attenuation in aortic wall and medial thickness was associated with less collagen fiber deposition (Figure 3C) and greater elastic fiber preservation in *Rock2*$^{+/-}$ mice compared with that of WT mice (Figure 3D). This correlated with decreased amount of hydroxyproline, an indicator of collagen fiber content, in the aortas of *Rock2*$^{+/-}$ mice compared with that of WT mice (Figure 3E). Furthermore, the level of desmosine and isodesmosine, which cross-links with elastin, was higher in aortas from *Rock2*$^{+/-}$ mice compared with that of WT mice after Ang II/L-NAME treatment (Figure 3F). Using the ratio of collagen to elastin as an index of extracellular matrix remodeling of the aorta, we found that WT mice have higher remodeling compared with that of *Rock1*$^{+/-}$ and *Rock2*$^{+/-}$ mice following Ang II/L-NAME treatment (Figure 3G). These results indicate that *Rock1*, and to a greater extent *Rock2*, are critical mediators of wall thickening and extracellular matrix remodeling of the aortic wall that could lead to aortic stiffening.

ROCK2 Mediates SMC Proliferation Through eEF1A1 Phosphorylation

To determine the mechanism by which ROCKs regulate vascular remodeling and stiffness, we hypothesized that phosphorylation of eEF1A1 by ROCK2 could be involved in aortic SMC proliferation and

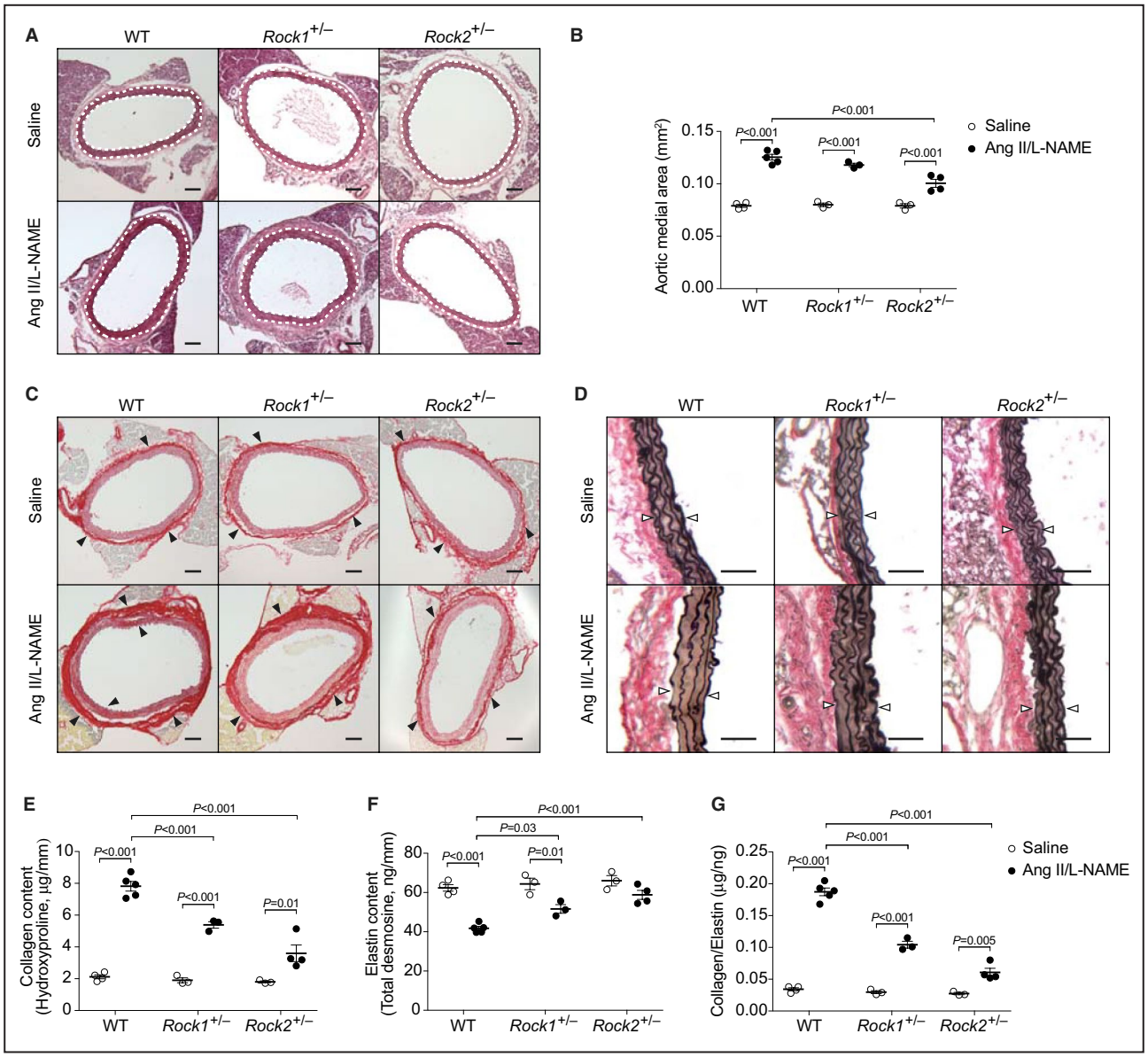

Figure 3. Morphology of aortas from Rho/Rho-associated coiled-coil containing kinase (*Rock)1*$^{+/-}$ and *Rock2*$^{+/-}$ mice with saline or Angiotensin II/L-N$^{\omega}$-nitroarginine methyl ester treatment.

A, Hematoxylin and eosin staining of aortas after saline or angiotensin II (Ang II)/L-N$^{\omega}$-nitroarginine methyl ester treatment for 4 weeks. The medial area is indicated by white dash lines. Scale bar represents 100 μm. **B**, Quantification of medial area from the aortic section of hematoxylin and eosin staining. **C**, Representative images of picrosirius red-stained aortic sections. Black arrowhead indicates collagen deposition. Scale bar represents 100 μm. **D**, Morphology of elastic fibers in elastin-stained aortic sections. White arrowhead indicates the distribution of elastic fibers. Scale bar represents 50 μm. Cross-linked (**E**) collagen and (**F**) elastin content in aortas were determined by measurement of hydroxyproline content and HPLC/MS detection of total desmosine (desmosine+isodesmosine). **G**, The ratio of collagen (hydroxyproline) to elastin (total desmosine) content in the aorta. Saline group: wild-type (n=4), *Rock1*$^{+/-}$ (n=3), and *Rock2*$^{+/-}$ (n=3). Ang II/ L-N$^{\omega}$-nitroarginine methyl ester group: wild-type (n=5), *Rock1*$^{+/-}$ (n=3), and *Rock2*$^{+/-}$ (n=4). Results are expressed as mean±SEM. *P* values were calculated using 1-way ANOVA with Tukey Honest Significant Difference test. Ang II indicates angiotensin II; L-NAME, L-N$^{\omega}$-nitroarginine methyl ester; *Rock*, Rho/Rho-associated coiled-coil containing kinase; and WT indicates wild-type.

hypertrophy. Previously, we have shown that ROCK2 can phosphorylate eEF1A1 at Thr^{432},[13] and eEF1A1 has been shown to play an important role in regulating the actin cytoskeleton.[23] Using an antibody against phospho-Thr^{432} of eEF1A1, we found that treatment with the ROCK inhibitor, Y-27632, decreased eEF1A1 phosphorylation in primary aortic SMC (Figure 4A). Compared with SMC treated with control or *Rock1* siRNA, eEF1A1 Thr^{432} phosphorylation was reduced in SMC treated with *Rock2* siRNA (Figure 4B).

To confirm that eEF1A1 Thr^{432} phosphorylation by ROCK2 contributes to ROCK2-mediated SMC proliferation and

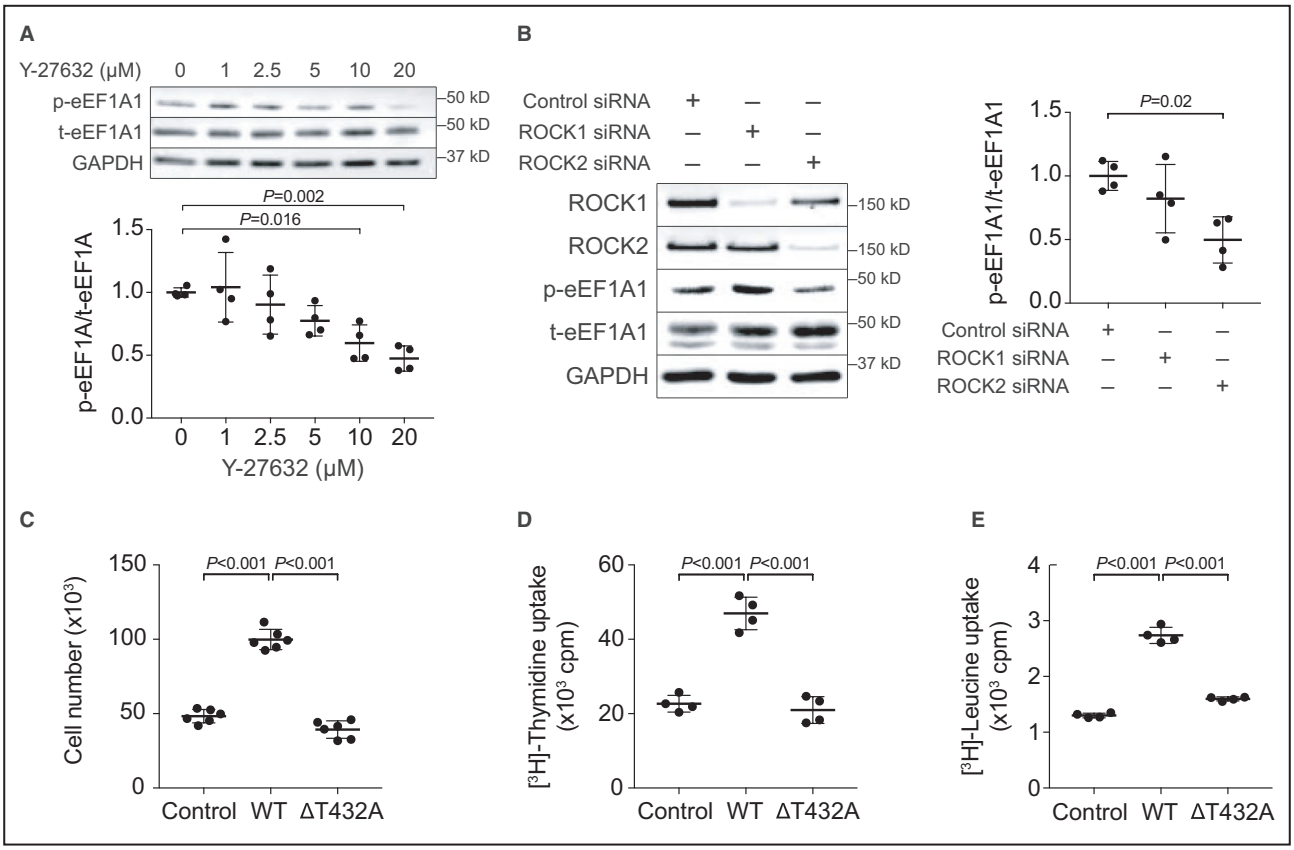

Figure 4. Phosphorylation of eEF1A1 by ROCK2 regulates SMC proliferation and protein synthesis.
A, Immunoblots showing eukaryotic elongation factor 1-alpha 1 (eEF1A1) Thr^{432} phosphorylation (p-eEF1A1) and total eEF1A1 (t-eEF1A1) in primary aortic smooth muscle cells (SMC) treated with increasing concentration of the ROCK inhibitor, Y-27632, for 24 hours. Densitometric analysis of eEF1A1 phosphorylation (p-eEF1A1/t-eEF1A1). n=4 cell isolates in each group. **B**, Immunoblots of wild-type SMC treated with control (scrambled), *Rock1*, or *Rock2* siRNA, n=4 cell isolates in each group. Cell proliferation was determined by (**C**) cell number and (**D**) [^{3}H]-thymidine uptake in response to 10% serum in SMC transfected with empty vector (control), wild-type eEF1A1, or mutant eEF1A1 (ΔT432A). SMC were synchronized to G0 phase with serum starvation for 16 hours before experiments. n=6 cell isolates for cell number and n=4 cell isolates for thymidine uptake. **E**, Protein synthesis was determined by [^{3}H]-leucine uptake. n=4 cell isolates. Results are expressed as mean±SEM. *P* values were calculated using 1-way ANOVA with Tukey Honest Significant Difference test. ROCK indicates Rho/Rho-associated coiled-coil containing kinase; siRNA, small interfering RNA; GAPDH, glyceraldehyde 3-phosphate dehydrogenase; and WT, wild-type.

hypertrophy, we made a mutant eEF1A1 (ΔT432A), which cannot be phosphorylated by ROCK2.[13] Compared with control vector, overexpression of WT eEF1A1 in SMC led to increased cell proliferation and protein synthesis, while overexpression of mutant eEF1A1 (ΔT432A) had no effect on SMC proliferation (Figure 4C through 4E). These results suggest that phosphorylation of Thr^{432} of eEF1A1 by ROCK2 mediates SMC proliferation and hypertrophy, which could contribute to medial SMC proliferation and wall thickening in the aorta.

ROCK2 Mediates Profibrotic Gene Expression

To determine the role of ROCK isoforms in Ang II-induced extracellular matrix remodeling, we first examined the expression of profibrotic genes in Ang II-stimulated primary aortic SMC with and without the ROCK inhibitor, Y-27632. Treatment with Ang II increased ROCK activity and upregulated TGF-β1 and collagen I protein and mRNA expression in SMC, which were substantially attenuated by Y-27632 (Figure 5A and 5B). Selective knockdown of *Rock1* or *Rock2* in SMC led to a comparable reduction in Ang II-induced TGF-β1 and collagen I protein expression (Figure 5C). Similarly, using MEF that were isolated from WT, *Rock1*$^{-/-}$ and *Rock2*$^{-/-}$ embryos, we found that the expression of collagen I, and the downstream effector of TGF-β1, CTGF, were both reduced in response to TGF-β1 stimulation (Figure 5D). These findings suggest that ROCK inhibition, and in particular, ROCK2 inhibition attenuates Ang II-induced TGF-β1 signaling and fibrosis, in part, through downregulation of TGF-β1 expression and its downstream profibrotic effectors, CTGF, and collagen I.

DISCUSSION

We have found that aortic ROCK activity increases with age and haploinsufficiency of *Rock1*, and to a greater extent, *Rock2*, confers protection against age-associated aortic stiffening. Using a pharmacologically-induced vascular stiffening model with Ang II/L-NAME, we found that hypertension, myocardial hypertrophy, aortic stiffening, and vascular remodeling were also reduced in hemizygous *Rock* mice, especially in *Rock2*$^{+/-}$ mice. The attenuation in aortic stiffening in *Rock2*$^{+/-}$ mice was accompanied by reduced vascular wall thickness, greater distensibility, less collagen deposition, and more preserved elastin content. In vitro, we showed that the phosphorylation of eEF1A1 by ROCK2 contributes to SMC proliferation and hypertrophy, which could account for the medial thickening of the aorta in older mice. Furthermore, the loss of *Rock2* led to decreased profibrotic gene expression. These findings indicate that ROCK2 is an important mediator of vascular remodeling and fibrosis, and suggest that ROCK could be a therapeutic target for age-associated aortic wall remodeling and stiffening.

Aortic stiffness is associated with impaired endothelial function and increased vascular tone.[24] An essential mediator of endothelial function and vasodilation is eNOS. The contribution of endothelial dysfunction in aortic stiffness is supported by higher blood pressure and aortic stiffness in eNOS knockout mice.[25] In our pharmacologically-induced vascular stiffening model, Ang II/L-NAME increased ROCK activity,[16,26] and increased ROCK activity has been shown to downregulate eNOS,[17] impair endothelial function,[27] and promote vascular remodeling.[14] The accelerated aortic stiffening model required the treatment of L-NAME, further highlighting the involvement of eNOS in the vascular stiffening process. Indeed, ROCK2 downregulates eNOS expression via phosphorylation of eEF1A1, which directly binds to eNOS mRNA and limits its mRNA stability.[13] The impaired endothelium-dependent dilation in aging cerebral arteries was reversed by selective sROCK2 inhibitor SLX-2119.[28] Consistent with these previous studies, we also found that eNOS mRNA level was decreased in the aortas of older WT and *Rock1*$^{+/-}$ mice but not in older *Rock2*$^{+/-}$ mice compared with that of younger corresponding mice. These findings suggest that ROCK2-mediated downregulation of eNOS and endothelial dysfunction may be one of the mechanisms by which ROCK2 mediates vascular stiffening and hypertension. Further studies using endothelial-specific ROCK isoform deletion in mice would be helpful in determining the mechanisms of endothelial ROCK2 in vascular stiffening.

Vascular aging is associated with enhanced contractile response to vasoconstrictors and increased myogenic tone. ROCK could increase blood pressure through their direct effects on SMC contraction via changes in actin cytoskeletal dynamics. ROCK phosphorylates myosin-binding subunit of MLC phosphatase and inhibits MLC phosphatase activity, leading to increased MLC phosphorylation, actomyosin interaction, and contraction.[7,29] The eEF1A mediates binding and cross-linking F-actin into non-contractile bundles.[30] Domain III of eEF1A has been shown to cross-link actin filaments with a unique binding rule that excludes other proteins from cross-linking F-actin into contractile bundles, such as phosphorylated MLC.[11] The binding of eEF1A to F-actin could negatively affect cellular contractility and alter cell shape by preventing actin-myosin interaction. Interestingly, the unphosphorylated form of eEF1A has been shown to bind to and bundle F-actin, whereas phosphorylated eEF1A at Thr^{432} by ROCK is unable to bind F-actin.[23] Thus, by phosphorylating eEF1A and preventing its interaction with F-actin, ROCK could induce SMC contraction by permitting the available F-actin to cross-link with phosphorylated MLC. Although both ROCK1 and ROCK2 can regulate MLC phosphatase, the ROCK2-eEF1A interaction may be more important for vascular contraction, which is reflected by the finding that knockdown of ROCK2, but not ROCK1, reduces the contractility in rat vascular smooth muscle cells (VSMC).[31] Moreover, the ROCK2-specific inhibitor, KD025, significantly inhibits the myogenic tone in mice at 2, 6 to 8, and 13 to 14 months of age via ROCK2-mediated Ca^{2+} sensitization.[32] Thus, these findings highlight the distinct effects of ROCK2 in mediating vascular contraction as well as age-related hypertension.

Epidemiological studies have shown that premenopausal women are protected against arterial stiffening compared with age-matched men.[33] Increased contractions to vasoconstrictor in aortas from male mice are attributable to higher in RhoA/ROCK activation in smooth muscles, independent of differences in the expression of RhoA or ROCK isoforms.[34] Basal activity of RhoA but not ROCK is higher in aortas of male mice and there is no difference in levels of ROCK1 and ROCK2 in aortas from male and female mice.[34] Interestingly, 17β-estradiol attenuates vascular contraction through inhibition of RhoA/ROCK activity.[35] The inhibitory effect of estrogen on RhoA/ROCK activity may be attributable to the activation of G protein-coupled estrogen receptors, leading to the downstream Epac/Rap1- and PKA-mediated RhoA/ROCK inhibition.[36] Our findings indicate that the PWV was lower in old female WT mice than in age-matched male mice. The haploinsufficiency of ROCK isoforms seems to exhibit similar protective effects on age-related vascular stiffness in both male and female mice.

Vascular thickening and remodeling are predominant structural changes that occur in vascular aging. Upregulation of ROCK2, but not ROCK1, is found in the media of pulmonary arteries from patients with idiopathic

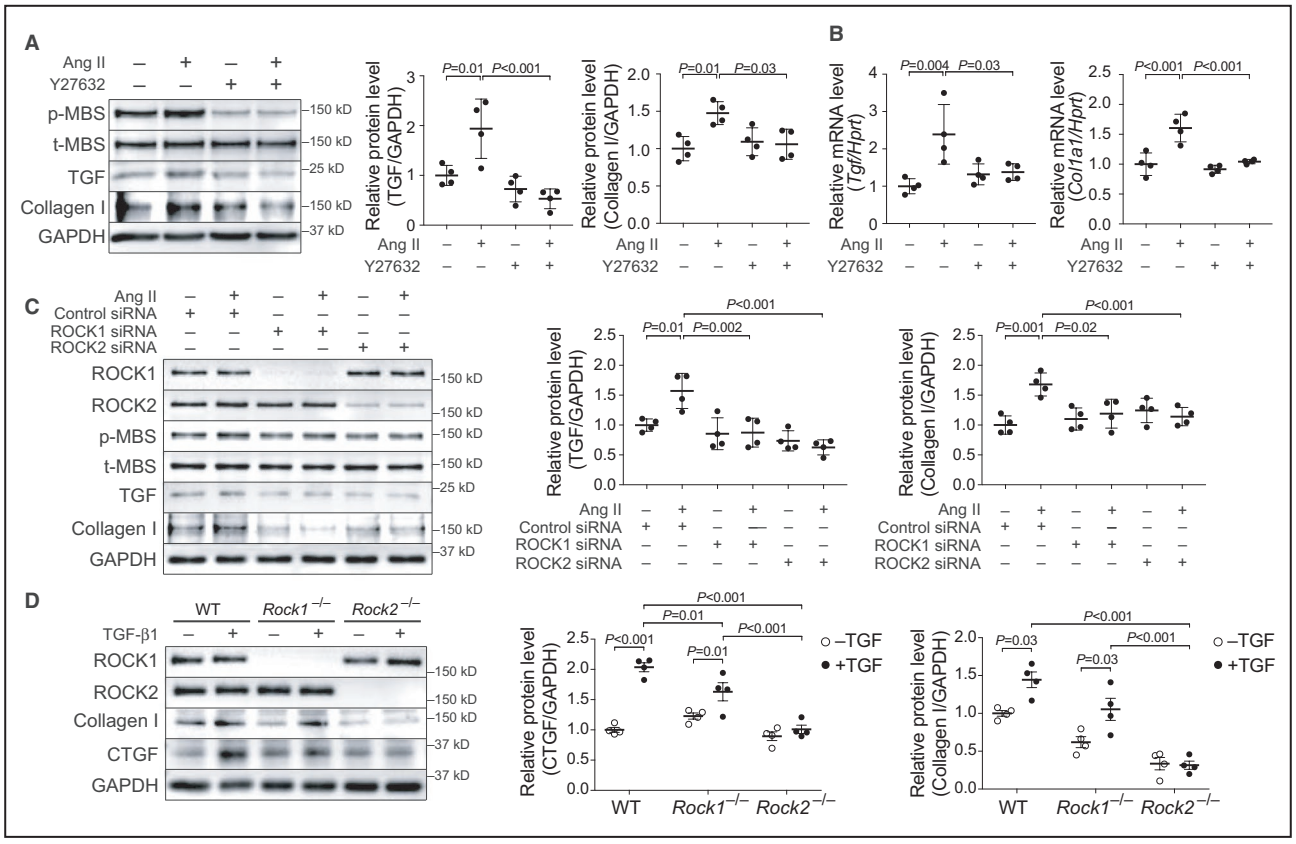

Figure 5. Regulation of transforming growth factor-β1 and collagen I expression by Rho/Rho-associated coiled-coil containing kinase (ROCK) isoforms.

A, Protein and (**B**) mRNA levels of transforming growth factor-β1 and collagen I in wild-type primary aortic smooth muscle cells (SMC) treated with Ang II (10 μmol/L) or Y-27632 (20 μmol/L) for 24 hours. n=4 cell isolates in each group. **C**, Representative immunoblots and densitometric quantification of transforming growth factor-β1 and collagen I in wild-type SMC treated with control (scrambled), *Rock1* or *Rock2* small interfering RNA. After transfection of small interfering RNA for 48 hours, SMC were stimulated with or without Ang II (10 μmol/L) for 24 hours, n=4 cell isolates in each group. **D**, Representative immunoblots and densitometric quantification of connective tissue growth factor and collagen I in wild-type, *Rock1*$^{-/-}$ or *Rock2*$^{-/-}$ mouse embryonic fibroblasts treated with transforming growth factor-β1 (10 ng/mL) for 24 hours; n=4 cell isolates in each group. Results are expressed as mean±SEM. *P* values were calculated using 1-way ANOVA with Tukey Honest Significant Difference test. Ang II indicates angiotensin II; CTGF, connective tissue growth factor; p-MBS indicates phosphorylated myosin-binding subunit; ROCK/*Rock*, Rho/Rho-associated coiled-coil containing kinase; siRNA, small interfering RNA; TGF, transforming growth factor; t-MBS, total myosin-binding subunit; GAPDH, glyceraldehyde 3-phosphate dehydrogenase; Hprt, hypoxanthine phosphoribosyltransferase; Col1a1, collagen type I alpha 1 chain; and WT, wild-type.

pulmonary arterial hypertension.[37] The hypoxia-induced VSMC proliferation and pulmonary arterial thickening are reduced in VSMC-specific ROCK2$^{+/-}$ mice, whereas the overexpression of ROCK2 in VSMC enhances both features of pulmonary arteries.[37] The arterial SMC from patients with pulmonary hypertension further confirms that ROCK2 is required for ERK1/2-mediated cell proliferation and vascular remodeling in pulmonary arteries.[37] These results support the notion that ROCK2 in VSMC regulates vascular remodeling through ERK-mediated proliferative signal, which may be a similar mechanism to ROCK2-mediated eEF1A1 phosphorylation-induced SMC proliferation in the present study.

We found a relatively intact aortic wall structure and relative maintenance of elastic fibers in *Rock2*$^{+/-}$ aortas after Ang II/L-NAME treatment. These observations suggest that Ang II/L-NAME-induced elastolysis may be attenuated by ROCK2 deficiency, suggesting ROCK2 could increase the activity of elastin-degrading enzymes in the vasculature. Indeed, pharmacological inhibition of ROCK decreases aortic elastin fragmentation, matrix metalloproteinase-2 activity, and vascular inflammation in Ang II-induced aneurysm animal models.[38,39] Our previous study also reported that leukocyte/macrophage ROCK1 is a mediator of vascular inflammation, neointima formation, and atherosclerosis.[14,40] However, the mechanisms by which ROCK regulates the production of elastolytic enzymes in vascular or inflammatory cells remains to be determined.

Although previous studies show that ROCK1 deletion mediates cardiovascular remodeling and fibrosis through transcriptional regulation of TGF-β1 and its downstream profibrotic genes,[14,15] the specific role of ROCK2 in vascular fibrosis is not entirely known. ROCK2, but not ROCK1, have been shown to mediate kidney fibrosis through TGF-β1–induced expression of CTGF and profibrotic genes via the proinflammatory transcription factor, nuclear factor-κB, in mesangial cells.[41] This observation agrees with our previous findings about the profibrotic effect of ROCK2 in cardiac fibroblasts.[16] The expression of ROCK2, but not ROCK1, is increased in activated cardiac fibroblasts after Ang II treatment and ROCK2 deletion in cardiac fibroblasts leads to a reduction in Ang II-induced cardiac fibrosis, as well as decreases in collagen and CTGF expression. Similarly, in this study, we showed that ROCK2 affects vascular stiffening and remodeling, in part, through TGF-β1 signaling pathways that control the expression of CTGF and collagen. Moreover, since the levels of Ang II[42] and TGF-β1[43] are elevated in circulation of aging animals and humans, these 2 factors could act as the inducers of vascular stiffness, or even the ROCK2 activators, which further highlight the importance of ROCK2 inhibition in alleviation of aging-related vascular stiffness.

In summary, using *Rock1* and *Rock2* haploinsufficient mice, we have shown that *Rock2* is the predominant mediator of vascular remodeling and stiffening that occurs with aging. Our findings suggest that ROCK2 may be a potential therapeutic target for the prevention of age-associated vascular disease.

ARTICLE INFORMATION

Received May 21, 2021; accepted August 23, 2021.

Affiliations

Division of Cell Regeneration and Transplantation, Department of Functional Morphology, Nihon University School of Medicine, Tokyo, Japan (Y.L.); Section of Cardiology, Department of Medicine, University of Chicago, IL (H.-C.T., N.S., J.K.L.); and Neurovascular Laboratory, Massachusetts General Hospital and Harvard Medical School, Boston, MA (H.K.).

Sources of Funding

This work was supported by National Institutes of Health (HL052233 and HL136962).

Disclosures

Dr Liao serves as a consultant for Esperion. The remaining authors have no disclosures to report.

Supplementary Material

Tables S1–S2

REFERENCES

1. Chirinos JA, Segers P, Hughes T, Townsend R. Large-artery stiffness in health and disease: JACC state-of-the-art review. *J Am Coll Cardiol*. 2019;74:1237–1263.
2. Safar ME. Arterial stiffness as a risk factor for clinical hypertension. *Nat Rev Cardiol*. 2018;15:97–105. doi: 10.1038/nrcardio.2017.155
3. Mitchell GF, Conlin PR, Dunlap ME, Lacourciere Y, Arnold JM, Ogilvie RI, Neutel J, Izzo JL Jr, Pfeffer MA. Aortic diameter, wall stiffness, and wave reflection in systolic hypertension. *Hypertension*. 2008;51:105–111. doi: 10.1161/HYPERTENSIONAHA.107.099721
4. Safar ME, Asmar R, Benetos A, Blacher J, Boutouyrie P, Lacolley P, Laurent S, London G, Pannier B, Protogerou A, et al. Interaction between hypertension and arterial stiffness. *Hypertension*. 2018;72:796–805. doi: 10.1161/HYPERTENSIONAHA.118.11212
5. Qiu H, Depre C, Ghosh K, Resuello RG, Natividad FF, Rossi F, Peppas A, Shen YT, Vatner DE, Vatner SF. Mechanism of gender-specific differences in aortic stiffness with aging in nonhuman primates. *Circulation*. 2007;116:669–676. doi: 10.1161/CIRCULATIONAHA.107.689208
6. Donato AJ, Machin DR, Lesniewski LA. Mechanisms of dysfunction in the aging vasculature and role in age-related disease. *Circ Res*. 2018;123:825–848. doi: 10.1161/CIRCRESAHA.118.312563
7. Maekawa M, Ishizaki T, Boku S, Watanabe N, Fujita A, Iwamatsu A, Obinata T, Ohashi K, Mizuno K, Narumiya S. Signaling from Rho to the actin cytoskeleton through protein kinases ROCK and LIM-kinase. *Science*. 1999;285:895–898. doi: 10.1126/science.285.5429.895
8. Yu B, Sladojevic N, Blair JE, Liao JK. Targeting Rho-associated coiled-coil forming protein kinase (ROCK) in cardiovascular fibrosis and stiffening. *Expert Opin Ther Targets*. 2020;24:47–62. doi: 10.1080/14728222.2020.1712593
9. Noma K, Goto C, Nishioka K, Hara K, Kimura M, Umemura T, Jitsuiki D, Nakagawa K, Oshima T, Chayama K, et al. Smoking, endothelial function, and Rho-kinase in humans. *Arterioscler Thromb Vasc Biol*. 2005;25:2630–2635. doi: 10.1161/01.ATV.0000189304.32725.bd
10. Noma K, Goto C, Nishioka K, Jitsuiki D, Umemura T, Ueda K, Kimura M, Nakagawa K, Oshima T, Chayama K, et al. Roles of Rho-associated kinase and oxidative stress in the pathogenesis of aortic stiffness. *J Am Coll Cardiol*. 2007;49:698–705. doi: 10.1016/j.jacc.2006.06.082
11. Liu G, Grant WM, Persky D, Latham VM Jr, Singer RH, Condeelis J. Interactions of elongation factor 1alpha with F-actin and beta-actin mRNA: implications for anchoring mRNA in cell protrusions. *Mol Biol Cell*. 2002;13:579–592.
12. Ohta K, Toriyama M, Miyazaki M, Murofushi H, Hosoda S, Endo S, Sakai H. The mitotic apparatus-associated 51-kDa protein from sea urchin eggs is a GTP-binding protein and is immunologically related to yeast polypeptide elongation factor 1 alpha. *J Biol Chem*. 1990;265:3240–3247. doi: 10.1016/S0021-9258(19)39759-5
13. Hiroi Y, Noma K, Kim HH, Sladojevic N, Tabit CE, Li Y, Soydan G, Salomone S, Moskowitz MA, Liao JK. Neuroprotection mediated by upregulation of endothelial nitric oxide synthase in Rho-associated, coiled-coil-containing kinase 2 deficient mice. *Circ J*. 2018;82:1195–1204. doi: 10.1253/circj.CJ-17-0732
14. Noma K, Rikitake Y, Oyama N, Yan G, Alcaide P, Liu P-Y, Wang H, Ahl D, Sawada N, Okamoto R, et al. ROCK1 mediates leukocyte recruitment and neointima formation following vascular injury. *J Clin Invest*. 2008;118:1632–1644. doi: 10.1172/JCI29226
15. Zhang Y-M, Bo J, Taffet GE, Chang J, Shi J, Reddy AK, Michael LH, Schneider MD, Entman ML, Schwartz RJ, et al. Targeted deletion of ROCK1 protects the heart against pressure overload by inhibiting reactive fibrosis. *FASEB J*. 2006;20:916–925. doi: 10.1096/fj.05-5129com
16. Shimizu T, Narang N, Chen P, Yu B, Knapp M, Janardanan J, Blair J, Liao JK. Fibroblast deletion of ROCK2 attenuates cardiac hypertrophy, fibrosis, and diastolic dysfunction. *JCI Insight*. 2017;2:e93187. doi: 10.1172/jci.insight.93187
17. Rikitake Y, Kim HH, Huang Z, Seto M, Yano K, Asano T, Moskowitz MA, Liao JK. Inhibition of Rho kinase (ROCK) leads to increased cerebral blood flow and stroke protection. *Stroke*. 2005;36:2251–2257. doi: 10.1161/01.STR.0000181077.84981.11
18. Liu PY, Liao JK. A method for measuring Rho kinase activity in tissues and cells. *Methods Enzymol*. 2008;439:181–189.
19. Mitchell GF. Effects of central arterial aging on the structure and function of the peripheral vasculature: implications for end-organ damage. *J Appl Physiol (1985)*. 2008;105:1652–1660. doi: 10.1152/japplphysiol.90549.2008
20. Fitch RM, Rutledge JC, Wang YX, Powers AF, Tseng JL, Clary T, Rubanyi GM. Synergistic effect of angiotensin II and nitric oxide synthase inhibitor in increasing aortic stiffness in mice. *Am J Physiol Heart Circ Physiol*. 2006;290:H1190–H1198. doi: 10.1152/ajpheart.00327.2005

21. Stegemann H, Stalder K. Determination of hydroxyproline. *Clin Chim Acta*. 1967;18:267–273. doi: 10.1016/0009-8981(67)90167-2
22. Mitchell GF, Guo CY, Benjamin EJ, Larson MG, Keyes MJ, Vita JA, Vasan RS, Levy D. Cross-sectional correlates of increased aortic stiffness in the community: the Framingham Heart Study. *Circulation*. 2007;115:2628–2636. doi: 10.1161/CIRCULATIONAHA.106.667733
23. Izawa T, Fukata Y, Kimura T, Iwamatsu A, Dohi K, Kaibuchi K. Elongation factor-1 alpha is a novel substrate of Rho-associated kinase. *Biochem Biophys Res Commun*. 2000;278:72–78.
24. Wallace SML, Yasmin, McEniery CM, Mäki-Petäjä KM, Booth AD, Cockcroft JR, Wilkinson IB. Isolated systolic hypertension is characterized by increased aortic stiffness and endothelial dysfunction. *Hypertension*. 2007;50:228–233. doi: 10.1161/HYPERTENSIONAHA.107.089391
25. Jung SM, Jandu S, Steppan J, Belkin A, An SS, Pak A, Choi EY, Nyhan D, Butlin M, Viegas K, et al. Increased tissue transglutaminase activity contributes to central vascular stiffness in enos knockout mice. *Am J Physiol Heart Circ Physiol*. 2013;305:H803–H810. doi: 10.1152/ajpheart.00103.2013
26. Kataoka C, Egashira K, Inoue S, Takemoto M, Ni W, Koyanagi M, Kitamoto S, Usui M, Kaibuchi K, Shimokawa H, et al. Important role of Rho-kinase in the pathogenesis of cardiovascular inflammation and remodeling induced by long-term blockade of nitric oxide synthesis in rats. *Hypertension*. 2002;39:245–250. doi: 10.1161/hy0202.103271
27. Nohria A, Grunert ME, Rikitake Y, Noma K, Prsic A, Ganz P, Liao JK, Creager MA. Rho kinase inhibition improves endothelial function in human subjects with coronary artery disease. *Circ Res*. 2006;99:1426–1432. doi: 10.1161/01.RES.0000251668.39526.c7
28. De Silva TM, Modrick ML, Dabertrand F, Faraci FM. Changes in cerebral arteries and parenchymal arterioles with aging: role of Rho kinase 2 and impact of genetic background. *Hypertension*. 2018;71:921–927. doi: 10.1161/HYPERTENSIONAHA.118.10865
29. Uehata M, Ishizaki T, Satoh H, Ono T, Kawahara T, Morishita T, Tamakawa H, Yamagami K, Inui J, Maekawa M, et al. Calcium sensitization of smooth muscle mediated by a Rho-associated protein kinase in hypertension. *Nature*. 1997;389:990–994. doi: 10.1038/40187
30. Yang F, Demma M, Warren V, Dharmawardhane S, Condeelis J. Identification of an actin-binding protein from dictyostelium as elongation factor 1a. *Nature*. 1990;347:494–496. doi: 10.1038/347494a0
31. Wang Y, Zheng XR, Riddick N, Bryden M, Baur W, Zhang X, Surks HK. ROCK isoform regulation of myosin phosphatase and contractility in vascular smooth muscle cells. *Circ Res*. 2009;104:531–540. doi: 10.1161/CIRCRESAHA.108.188524
32. Bjorling K, Joseph PD, Egebjerg K, Salomonsson M, Hansen JL, Ludvigsen TP, Jensen LJ. Role of age, Rho-kinase 2 expression, and G protein-mediated signaling in the myogenic response in mouse small mesenteric arteries. *Physiol Rep*. 2018;6:e13863. doi: 10.14814/phy2.13863
33. Weng C, Yuan H, Yang K, Tang X, Huang Z, Huang L, Chen W, Chen F, Chen Z, Yang P. Gender-specific association between the metabolic syndrome and arterial stiffness in 8,300 subjects. *Am J Med Sci*. 2013;346:289–294. doi: 10.1097/MAJ.0b013e3182732e97
34. Nuno DW, Korovkina VP, England SK, Lamping KG. RhoA activation contributes to sex differences in vascular contractions. *Arterioscler Thromb Vasc Biol*. 2007;27:1934–1940. doi: 10.1161/ATVBAHA.107.144675
35. Yang E, Jeon SB, Baek I, Chen ZA, Jin Z, Kim IK. 17beta-estradiol attenuates vascular contraction through inhibition of RhoA/Rho kinase pathway. *Naunyn Schmiedebergs Arch Pharmacol*. 2009;380:35–44.
36. Yu X, Zhang Q, Zhao Y, Schwarz BJ, Stallone JN, Heaps CL, Han G. Activation of G protein-coupled estrogen receptor 1 induces coronary artery relaxation via Epac/Rap1-mediated inhibition of RhoA/Rho kinase pathway in parallel with PKA. *PLoS One*. 2017;12:e0173085. doi: 10.1371/journal.pone.0173085
37. Shimizu T, Fukumoto Y, Tanaka S, Satoh K, Ikeda S, Shimokawa H. Crucial role of ROCK2 in vascular smooth muscle cells for hypoxia-induced pulmonary hypertension in mice. *Arterioscler Thromb Vasc Biol*. 2013;33:2780–2791. doi: 10.1161/ATVBAHA.113.301357
38. Wang Y-X, Martin-McNulty B, da Cunha V, Vincelette J, Lu X, Feng Q, Halks-Miller M, Mahmoudi M, Schroeder M, Subramanyam B, et al. Fasudil, a Rho-kinase inhibitor, attenuates angiotensin II-induced abdominal aortic aneurysm in apolipoprotein E-deficient mice by inhibiting apoptosis and proteolysis. *Circulation*. 2005;111:2219–2226. doi: 10.1161/01.CIR.0000163544.17221.BE
39. Tsai SH, Huang PH, Peng YJ, Chang WC, Tsai HY, Leu HB, Chen JW, Lin SJ. Zoledronate attenuates angiotensin II-induced abdominal aortic aneurysm through inactivation of Rho/ROCK-dependent JNK and NF-kappaB pathway. *Cardiovasc Res*. 2013;100:501–510.
40. Wang HW, Liu PY, Oyama N, Rikitake Y, Kitamoto S, Gitlin J, Liao JK, Boisvert WA. Deficiency of ROCK1 in bone marrow-derived cells protects against atherosclerosis in LDLR$^{-/-}$ mice. *FASEB J*. 2008;22:3561–3570.
41. Nagai Y, Matoba K, Kawanami D, Takeda Y, Akamine T, Ishizawa S, Kanazawa Y, Yokota T, Utsunomiya K, Nishimura R. ROCK2 regulates TGF-beta-induced expression of CTGF and profibrotic genes via NF-kappaB and cytoskeleton dynamics in mesangial cells. *Am J Physiol Renal Physiol*. 2019;317:F839–F851.
42. Yoon HE, Kim EN, Kim MY, Lim JH, Jang IA, Ban TH, Shin SJ, Park CW, Chang YS, Choi BS. Age-associated changes in the vascular renin-angiotensin system in mice. *Oxid Med Cell Longev*. 2016;2016:6731093. doi: 10.1155/2016/6731093
43. Carlson ME, Conboy MJ, Hsu M, Barchas L, Jeong J, Agrawal A, Mikels AJ, Agrawal S, Schaffer DV, Conboy IM. Relative roles of TGF-beta1 and Wnt in the systemic regulation and aging of satellite cell responses. *Aging Cell*. 2009;8:676–689.

SUPPLEMENTAL MATERIAL

Table S1. List of primary antibodies

Target antigen	Vendor or Source	Catalog #	Working concentration
ROCK1	BD Biosciences	611136	1:1000 (250 ng/ml)
ROCK2	BD Biosciences	610623	1:1000 (250 ng/ml)
Phos-MYPT1 (p-MBS, Thr850)	Millipore	36-003	1:1000 (1000 ng/ml)
Myosin Phosphatase (t-MBS)	Biolegend	925101	1:1000 (N/A)
beta-actin	Proteintech	66009	1:5000 (86 ng/ml)
Phospho-eEF1A1	Dr. James K. Liao	N/A	1:1000 (N/A)
EF-1 α1/2	Santa Cruz	377439	1:1000 (200 ng/ml)
GAPDH	Cell Signaling Technology	2118	1:5000 (N/A)
TGFb1	Santa Cruz	sc-146	1:1000 (100 ng/ml)
COL1A1	Santa Cruz	sc-8784	1:1000 (100 ng/ml)
CTGF	Santa Cruz	365970	1:1000 (200 ng/ml)

Table S2. List of primers used in quantitative real-time PCR

Gene name	Forward Primer (5'->3')	Reverse Primer (5'->3')
Tgfb1	GAAGCGGACTACTATGCTAAA	CCCGAATGTCTGACGTATTG
Col1a1	CAATGGTGCTCCTGGTATTG	CACCAGTGTCTCCTTTGTTG
Rock1	GGAGATGTGTACAGAGCAGAAA	GAAAGTGGTAGAGGGTAGGAATG
Rock2	ACAGATGAAAGCGGAAGACTATG	TGAACTACCCAGGGACTGTT
Nos3	GACAGACTACACGACATTGAG	ATGGTCCAGTTGGGAGCATC
Hprt	AGTGTTGGATACAGGCCAGAC	CGTGATTCAAATCCCTGAAGT